

SLAC-PUB-9565
September, 2002

A Liquid Hydrogen Target for the Precision
Measurement of the Weak Mixing Angle in
Møller Scattering at SLAC

J. Gao¹, K. K. Gusstafsson², R. Carr, C. E. Jones, G. M. Jones,
R. D. McKeown, A. Scott

*W. K. Kellogg Radiation Laboratory, California Institute of Technology
Pasadena, CA 91125, USA*

R. Boyce, W. Burgess, A. Candia, W. Kaminskas, G. Oxoby,
T. Weber, J. G. Weisend II

Stanford Linear Accelerator Center, Stanford, CA 94309, USA

¹Corresponding author

²Current mailing address: Helsinki Institute of Physics, P.O. Box 64, FIN-00014
University of Helsinki, Finland

A Liquid Hydrogen Target for the Precision Measurement of the Weak Mixing Angle in Møller Scattering at SLAC

J. Gao¹, K. K. Gustafsson², R. Carr, C. E. Jones,
R. D. McKeown, A. Scott

*W. K. Kellogg Radiation Laboratory, California Institute of Technology,
Pasadena, CA 91125, USA*

P. L. Anthony, R. F. Boyce, W. Burgess, A. Candia,
W. Kaminskis, G. Oxoby, M. P. Racine, T. Weber,
J. G. Weisend II

Stanford Linear Accelerator Center, Stanford, CA 94309, USA

Abstract

A 150 cm long liquid hydrogen target has been built for the SLAC End Station A E158 experiment. The target loop volume is 55 liters, and the maximum target heat load deposited by the electron beam is ~ 700 W. The liquid hydrogen density fluctuation with full beam current (120 Hz repetition rate, 6×10^{11} electrons/spill) on target is well below 10^{-4} level, which fulfills the requirement for a precision measurement of the weak mixing angle in the polarized electron-electron scattering process.

Key words: Hydrogen Target, Parity Violating, Density fluctuation
PACS: 25.30.Bf, 14.60.Cd, 12.15.Mm

¹ Corresponding author. Email address: jgao@krl.caltech.edu

² Current mailing address: Helsinki Institute of Physics, P.O. Box 64, FIN-00014 University of Helsinki, Finland

1 Introduction

Parity violating Møller scattering provides a unique method to study weak neutral current interactions. The cross section asymmetry (A_{LR}) using left or right handed incident electrons arises from the interference of neutral weak current and electromagnetic current. At $Q^2 \ll M_Z^2$, a precision measurement of A_{LR} , and eventually the weak mixing angle $\sin^2 \theta_W$, can test the electroweak theory at the quantum loop level away from the Z^0 resonance and probe new physics beyond the standard model at the TeV scale.

The SLAC E158 experiment [1] is to measure $\sin^2 \theta_W$ at $Q^2 \sim 0.03$ (GeV/c)² using the 45/48 GeV polarized electron beam scattering off unpolarized electrons in a liquid hydrogen target. The asymmetry for this process is $\sim 10^{-7}$. In order to determine $\sin^2 \theta_W$ at a 0.3% level the asymmetry must be measured to a few parts per billion (ppb).

The 45/48 GeV pulsed beam from the SLAC accelerator has a maximum repetition rate of 120 Hz with a maximum of $\sim 6 \times 10^{11}$ electrons per pulse. That is, the maximum beam current is $12 \mu\text{A}$. In order to accomplish the measurement with a reasonable amount of beam time, the luminosity has to be high enough so that the pulse-to-pulse asymmetry width is at $1 - 2 \times 10^{-4}$ level. This leads to a target length of about 150 cm, and maximum beam heat load of ~ 700 W. In addition, the heat load generated by the pump and by heat leaks are estimated to be 200 W and 100 W, respectively. Thus, the heat exchanger must be able to provide 1,000 W of cooling power. The target density fluctuations need to be small compared to the statistical fluctuation of the scattered electrons.

A 150 cm long liquid hydrogen target has been built by a joint collaboration of Caltech and SLAC. Compared to the cryogenic target used at MIT-Bates [2] and at Jefferson Lab [3], this target has a large volume (55 liters) and high power (1 kW). It has been operational since February 2000 and meets the stringent requirements of the E158 experiment.

2 Description of the liquid hydrogen target

The E158 liquid hydrogen target system can be divided into four major components: coolant supply system, gas handling system, target loop, and target control and monitoring system. The gas panel, scattering chamber and the distribution box are located inside End Station A, while the refrigerator, hydrogen ballast tank and hydrogen tube trailer are outside of End Station A.

The target loop is located inside a scattering chamber. The 75,000 liters ballast tank serves as the hydrogen gas supply and also maintains a constant pressure inside the target loop. The gas panel controls gas flow in both directions. The coolant, 11 K cold helium gas generated by the refrigerator, is delivered to the target loop via a distribution box inside End Station A.

2.1 Coolant supply

The SLAC Sulzer/CTI 4000 helium refrigerator [4] is used to provide the necessary coolant. It supplies 50 psia, ~ 12 K helium gas, and can provide up to 1 kW cooling for the hydrogen target. The coolant is delivered from the refrigerator to the distribution box located in End Station A via a 72 meter long Triax flexible transfer line manufactured by Kabelmetal. This Triax transfer line contains a 10 mm i.d. tube for the supply flow and an annular space for the return flow. The two flows are separated from each other and from the outside environment by vacuum spaces. Two 23 mm i.d. vacuum insulated transfer lines link the target heat exchanger and the distribution box to supply and return coolant. Inside the distribution box there is an additional 500 W trim heater that can fine tune the coolant temperature.

2.2 Gas handling system

A schematic of the gas handling system is shown in Figure 2. The central element of the system is the main gas panel. The boundaries of the valve panel are illustrated with a dashed line in Figure 2. A number of manually operated and pneumatic valves constitute the main plumbing elements. Each valve is equipped with two micro-switches to monitor its status. In addition, there are pressure gauges, pressure transmitters, check valves, relief valves and rupture disks. The valves and target loop are linked by 2" stainless steel tubing. The distance between the target loop and the vent line is about 50'. Following the standard operating procedures [5], a target operator can pump and purge the target loop, fill the target loop with hydrogen or helium gas, and liquefy hydrogen in the target loop. During the hydrogen liquefying process the 75,000 liter ballast tank provides hydrogen gas. When needed, a tube trailer can supply hydrogen gas to the ballast tank. Once the target loop is filled with liquid hydrogen, the ballast tank serves as a buffer and maintains a constant pressure in the target loop.

On the valve panel there are redundant burst discs so that in the event of excessive pressure in the loop the hydrogen would escape through a 100 mm i.d. pipe. In the event of a catastrophic failure (vacuum is compromised, for example), the plumbing system can relieve the hydrogen quickly enough that

the maximum build-up pressure in the target loop is ~ 40 psia, less than half of the test pressure of the loop. If the liquid hydrogen is dumped in into the scattering chamber, the resulting hydrogen gas will vent through a 160 mm i.d. pipe. The vent lines are continuously purged with nitrogen gas to avoid the formation of explosive mixtures during hydrogen venting.

2.3 Scattering chamber and target loop

Figure 3 displays the schematic layout of the scattering chamber which houses the target loop and provides vacuum insulation.

The oblate spherical scattering chamber has a diameter of roughly 2 m and a height of 2 m. It is made of aluminum. Above the scattering chamber there is an external frame. The target loop hangs from that external frame, while the frame rests on 3 linked motorized jacks. These jacks allow the target loop to be lifted up to 15 cm out of the beam line. When the target loop is in its down position, its two aluminum flanges rest on two anvils and therefore target loop position relative to the beam line is fixed. These anvils are 1/8" thick stainless steel plates so the contact area is very small. Inside the scattering chamber there is also a table holding solid targets. The target loop can be moved vertically, and the solid target table can be moved horizontally by remote control. A hardware interlock assures that the solid target table can only be moved in if the target loop is out of the beam line, and vice versa. The scattering chamber has feedthroughs for the hydrogen gas line, helium transfer line, and for electric wiring of the temperature sensors and target heater.

The target loop is illustrated in Figure 4. The target cell is made of a 3" i.d., 1/4" wall 6061 T-6 aluminum pipe approximately 1.5 m long. Two explosion-bonded aluminum-to-stainless transition pieces with 3 3/8" conflat surfaces are used to connect the target cell to the rest of the target loop which is made of stainless steel. The target cell tube is capped off with two thin windows at both the upstream and downstream ends. The windows are made of 0.010" thick 1100 aluminum and are soft soldered to aluminum flanges which attach to the target cell. The target cell windows have a 3" radius of curvature. The body of the heat exchanger and the pump house are both made of 304 stainless steel.

Eight mesh discs machined from aluminum plate are mounted inside the target cell. These discs are oriented perpendicular to the beam direction and have a 1.5" diameter hole in the center to provide enough clearance around the beam axis. In addition, each disk has an open slot with a 45° opening angle. A schematic diagram of four successive discs is shown in Figure 5. The second disc has the slot diametrically opposed to the first, the third disc's slot is

opposite the second but offset by 45° , the fourth is diametrically opposed to the third disc's slot, and so on. The disc spacing is chosen randomly between four and eight inches to avoid resonances that might move fluid into the interaction region in phase with the beam pulses. The purpose of the wire mesh is to introduce turbulence of about the beam spot size ($\sim 1 - 2$ mm) as well as transverse flow in the target cell region, so that unheated liquid hydrogen can be mixed into the beam volume thoroughly, and therefore liquid hydrogen density fluctuation due to beam heating can be minimized [7].

The pump consists of two impellers sandwiched between three stators. It generates flow opposite to the beam direction in the target cell. Two conically shaped flow diverters located upstream and downstream of the stators complete the pump design. These pump components are all made of 6061 aluminum and they are connected to a stainless steel housing at a section on the inner surface of the top 14.5" conflat flange of the pump house. The power source of the target pump is a 2 hp 3-phase brushless electrical motor. This pump motor is located inside a can on top of the scattering chamber as shown in Figure 3. The $5/8$ " diameter shaft of the motor is connected via a flexible coupling to the $3/4$ " diameter stainless steel shaft of the pump. The motor runs in a hydrogen atmosphere at room temperature. A piece of G10 is used as a plug between the upper parts of the pump house and the lower parts of the tube leading up to the motor can. The plug prevents liquid hydrogen from splashing onto warmer components and maintains a temperature gradient from the room temperature environment to the cryogenic hydrogen. If splashing took place then it could give rise to pressure surges. The speed of the motor can be varied continuously between 0 and 60 Hz. Three identical magnetic rings are mounted around the pump shaft, and a stationary pickup coil in their vicinity generates sine wave signals which have the pump speed information.

The counter-flow heat exchanger is a 80 cm long copper coil with an outer diameter of ~ 11 cm. The coil is made of $3/8$ " o.d. copper tubing with .081" wall thickness wound into 42 turns. The copper coil is located inside a stainless steel housing made from a 6.75" CF full nipple. The total length of the copper tubing is 12.3 m. For heat exchange, the coolant inlet (outlet) is at the lower (upper) end of the heat exchanger. The cooling capacity of this heat exchanger is limited by the coolant flow. The coolant inlet temperature is typically 14 K while the return temperature is about 20 K.

A heater is located downstream of the heat exchanger inside the target loop. The target heater is made of nichrome (80% nickel, 20% chromium) wire wrapped on a G10 support structure. The wire leads between the support structure and the CF feedthrough as well as the leads from the outside of the target loop to feedthroughs on the wall of the scattering chamber are insulated using single bore radiation hard ceramic beads. The target heater

has a resistance of 1Ω , and is powered by a 1 kW Sorenson DCS33-33E power supply.

2.4 Target control and monitoring

A schematic of the target control is shown in Figure 6. The "hub" of the target control and monitoring is a PC running Windows NT. The PC is equipped with three interface cards: a PCI-GPIB card, a PCI-MIO card, and a PCI-DIO card. The PCI-GPIB card talks to the GPIB devices, including a Lakeshore 218S temperature monitor and a HP34401A multimeter. The PCI-MIO card can read/generate analog signals to monitor/control devices. The PCI-DIO card reads the digital signals (valve status) of the micro-switches on the valve panel. The target control software is written using National Instruments LabVIEW 5.1 [8]. The target operator monitors the target and gives commands via the graphical user interface provided by LabVIEW. Generally, the control software scans all the devices and updates once every two seconds. The target control computer also sends necessary information via internet to the refrigerator control computer. In addition, the target control software hosts a web site which broadcasts the display of the target control software.

The Cernox CX-1070-AA-4L temperature sensors are used to monitor temperatures of the target loop and the coolant. These 4-lead sensors are calibrated from 4 K to 325 K. The accuracy for cryogenic temperature measurement is ~ 10 mK. Two sensors (one of them is spare) are mounted at each of the four locations on the target loop: before (labeled "Tpi") and after the pump (Tpo); before (Thi) and after (Tho) the target heater. A drawing of one of the target loop temperature sensor feedthroughs is shown in Figure 7. In addition, four Cernox sensors are mounted on copper clamps embracing the outside of the heat exchanger inlet/outlet tubing to monitor the coolant inlet/return temperature. At each location there are two sensors, one sends signals to the target control system and the other sends signals to the CTF4000 refrigerator monitoring system. Since these four sensors are not directly exposed to the coolant, the readings from them are not the exact temperature of the coolant. In fact, the readings of these sensors are higher than the loop temperature. The leads of all sensors are connected to a feedthrough flange mounted on the scattering chamber. Individually shielded twisted pairs are used to connect the leads from the outside of the feedthrough to the Lakeshore 218S temperature monitor which is located in the counting house.

The pump speed is monitored with a tachometer. The tachometer pickup coil generates a sine wave signal which has the same frequency as the pump speed. The sine wave signal is then sent to the HP34401A multimeter to read out the frequency.

Two microswitches are mounted on each valve on the gas panel in order to monitor the valve status. The TTL signals generated by the microswitches are sent to the digital input channels of the PCI-DIO card. One can determine four possible valve states from the two independent TTL signals of each valve: open, closed, partially open and power failure.

The electron beam going through the target is measured by a beam current monitor (BCM) located on the beamline upstream of the target. The generated 0-10 V analog signal is sent to an analog input channel of the PCI-MIO card and converted to beam current reading.

A 0-5 V DC signal from the pump motor controller that is proportional to the pump motor current is sent to an analog input channel of the PCI-MIO card, where it is converted to pump motor current reading.

The target gas handling system uses Omega PX880 and Omega PX771 pressure transmitters which are located on the gas panel to measure the gas pressure. The 4-20 mA output current signals are transformed to 2-10 V voltage signals, sent to the analog input channels of the PCI-MIO card, and then converted into pressure readings.

The vacuum of the scattering chamber is monitored by a Leybold Combivac CM 31 vacuum gauge which has a thermocouple TR211 sensor and a cold cathode Penningvac PR35 sensor. The analog outputs (0-10 V) from these two sensors are sent to the analog input channels of the PCI-MIO card and then converted to vacuum pressure readings.

The Sorenson DCS33-33E power supply used by the target heater has a maximum output power of 1 kW (33 V and 33 A). The output current and voltage are remotely controlled with two 0-10 V signals set by the analog output channels of the PCI-MIO card. When the computer/crate hangs up or is unavailable, a control box is switched on to manually control the target heater power supply. This control box has the analog signals from the PCI-MIO card, and it itself generates two manually adjustable 0-10 V analog signals as well. Two 0-10 V analog outputs are connected to the heater power supply. The setting of a switch determines whether the analog output signals come from the PCI-MIO card or the control box.

3 Operational experience

3.1 Helium gas

The target system was first tested with 20 K helium gas in the fall of 2000. The results indicate that the target loop was leak tight, the pump worked as expected, and the heat exchanger could remove 1 kW heat at 14 K. The total heat deposited by static heat leaks and pump work was estimated to be less than 100 W. With quartz windows placed on the beam line flanges, it was found that the target was aligned to better than 0.4 mm relative to the ideal beam axis when the target was both cold and under vacuum. The target was repeatedly raised and lowered and the alignment of the target was reproducible within 0.08 mm. This is well within the design requirements.

By measuring the temperature difference across the heater for different heater power settings and different pump speed, one can study the pump efficiency and flow velocity using the following equations:

$$Q = C_p \dot{m} \Delta T \quad (1)$$

$$= C_p \rho(P, T) f V \epsilon \Delta T \quad (2)$$

$$= C_p \rho(P_0, T_0) f V \epsilon \frac{\rho(P, T)}{\rho(P_0, T_0)} \Delta T \quad (3)$$

$$= C_p \rho(P_0, T_0) f V \epsilon \Delta T_c, \quad (4)$$

where

Q : heater power

C_p : heat capacity

\dot{m} : mass flow rate

ΔT : temperature difference across the heater

$\rho(P, T)$: helium gas density

V : pump volume, about 1.6 liter

ϵ : pump efficiency

ΔT_c : temperature difference across the heater corrected for different helium gas density.

Figure 8 shows the ΔT_c for various pump speed and target heater power settings. The slope of each line gives the pump efficiency. Considering the fact that the target cell diameter is 3", one can calculate the flow speed along the beam line in the target cell (Figure 9).

The heat exchange rate for a counter-flow heat exchanger can be written as:

$$Q = U \Delta T_{LM} \quad (5)$$

$$\Delta T_{LM} = (\Delta T_o - \Delta T_i) / \ln(\Delta T_o) / (\Delta T_i) \quad (6)$$

$$U^{-1} = (h_t A_t)^{-1} + (h_c A_c)^{-1} \quad (7)$$

$$h = \frac{0.023 C_p G^{0.8} \eta^{0.2}}{(\eta C_p / \lambda)^{0.6} D_e^{0.2}}, \quad (8)$$

where

Q [W/s]: heat exchange rate

U [W/K]: heat exchange coefficient

ΔT_{LM} [K]: log mean temperature difference, ΔT_o and ΔT_i are the difference between the coolant and the target fluid temperature at the inlet and outlet

h_t, h_c [W/cm²-K]: heat exchange coefficients per unit area for target fluid and coolant

A_t, A_c [cm²]: heat exchange area at the target side and the coolant side

C_p [J/g-K]: heat capacity

G [g/s-cm²]: mass flow rate per unit area

η [g/cm-s]: viscosity

λ [W/cm-K]: thermal conductivity

D_e [cm]: effective diameter for heat exchange.

Since the heat exchange rate, flow rate, and temperature at all locations are known, one can deduce the heat exchange coefficient from the measurements. Figure 10 shows the measured heat exchange coefficient vs. calculation. One can see that the heat exchanger performs better than the above computed estimate.

3.2 *Liquid hydrogen*

Hydrogen gas was first successfully liquefied in the target loop in February, 2001. Although this target loop has a large volume (55 liters), it takes only 6 to 8 hours to fill the target with liquid hydrogen. The target loop is connected to a 75,000 liter ballast tank which is in turn supplied by the high-pressure hydrogen tube trailer. After the target loop is filled with hydrogen, the ballast tank maintains the loop pressure at a constant value (typically 21 psia). The initial 1 hp pump motor was not powerful enough to keep up the pump speed. It could suddenly slow down and cause spillage of liquid hydrogen into the warmer parts of the loop. As a result, there would be a pressure spike followed by an unwanted vent. pressurize and vent. The problem was solved by replacing the 1 hp pump motor with a 2 hp motor.

The total heat load in the target loop is kept constant by compensating with the target heater for changes in the electron beam current. At the same time,

the trim heater located in the coolant distribution box is automatically controlled so that the helium temperature at the inlet to the target heat exchanger is always constant. With these feedback loops in operation, the liquid hydrogen temperature varies no more than 150 mK over the course of one hour. In the summer of 2001, the maximum target heater power was set to 670 W, indicating the target could stand a maximum beam current of at least $\sim 11 \mu\text{A}$. In spring of 2002, the typical beam current on the liquid hydrogen target was about $11.5 \mu\text{A}$.

4 Density fluctuation study

When the electron beam pulse hits the target, the density of the liquid hydrogen volume along the beam path is reduced during the beam pulse due to the heat deposited by the beam. If there is noise in the electron beam parameter (beam radius, for example), the target density reduction will be random. Therefore, the target density will fluctuate from pulse to pulse. As a result, the detector signal contains a noise imposed by the randomly fluctuating target density, and the width of the pulse-to-pulse detector signal asymmetry is increased.

By introducing transverse flow and turbulence in the target cell region, the amount of liquid hydrogen heated by the beam can be mixed with the surrounding liquid between the beam pulses, and density reduction can be eased. If the mixing is not thorough, the random residual density reduction will reduce the detector yield of the next beam pulse randomly, and add to the density fluctuation. This effect is considered small for the E158 target, because the maximum repetition rate at SLAC is 120 Hz, so the time interval between two consecutive pulses is about 8 ms. The beam radius is 1-2 mm. The fluid in the target loop is highly turbulent. A 0.5 m/s transverse flow speed is sufficient to move the liquid volume heated by the beam out of the beam line. However, if the target pump speed is too low, the contribution to the total density fluctuation may be visible. Unlike target density fluctuation generated by beam heating during the beam pulse, the random residual density reduction does not generate a false physics asymmetry since the helicity of each beam pulse is chosen randomly.

Target density fluctuation not only increases the total amount of beam time to measure the physics asymmetry to a certain accuracy, but density fluctuation due to beam heating during the pulses also creates a false asymmetry in the measurement if there is a non-zero, helicity correlated beam spot size asymmetry. To probe target density fluctuation, one can look for the correlations between the asymmetries in the Møller detector and the luminosity detector [1], as a density change will change both asymmetries in the same amount.

Assuming target density fluctuation is the only common mode noise in the Møller and luminosity signals, the asymmetries in the Møller detector A_{Moller} and the luminosity detector A_{lumi} after regression can be parametrized as

$$A_{Moller} = A_{Moller}^0 + A_\rho \quad (9)$$

$$A_{lumi} = A_{lumi}^0 + A_\rho \quad (10)$$

with A_ρ is the target density asymmetry, A_{Moller}^0 and A_{lumi}^0 the asymmetries in the Møller detector and the luminosity detector with target density ρ kept constant. Since A_{Moller}^0 and A_{lumi}^0 are uncorrelated, if one defines

$$A_+ = A_{Moller} + A_{lumi} \quad (11)$$

$$A_- = A_{Moller} - A_{lumi} \quad (12)$$

then,

$$\Sigma_+^2 - \Sigma_-^2 = 4\Sigma_\rho^2 \quad (13)$$

with Σ_+ and Σ_- the RMS of A_+ and A_- . The RMS of A_ρ , Σ_ρ therefore gives the upper limit of the target density fluctuation.

Figure 11 displays measured Σ_ρ for different runs with 120 Hz repetition rate, 6×10^{11} electrons per spill, and 1.0 mm beam radius. The data is from the E158 physics run I taken in Spring, 2002. Except the three data points obtained with skew quad [9] off, the rest data points are for normal production runs. Initial data analysis indicates that beam spot size jitter is significantly increased if the skew quad is turned off, and the common mode noise is increased by a factor of more than 2. One can conclude from Figure 11 that for all the normal production runs listed in Figure 11, the target density fluctuation is below 65 ppm, which is very small compared to the grand averaged Møller detector asymmetry width (~ 200 ppm). A further detailed analysis and study of the target density fluctuation has been planned and results will be published later.

5 Conclusion

A large volume, high power liquid hydrogen target has been constructed for the E158 experiment at SLAC. The target has been used successfully for taking physics data. With the full beam current (120 Hz repetition rate, 6×10^{11} electrons/spill) on target and 1.0 mm beam radius, the upper limit of the

target density fluctuation is 6.5×10^{-5} for normal production runs, which fulfills the requirement for a precision measurement of the weak mixing angle in the polarized electron-electron scattering process.

Acknowledgments

This project would not have been accomplished without the dedicated, unconditional help of the SLAC Experimental Facilities Department. It is supported by DOE contract DE-AC03-76SF00515 and NSF grant PHY-0071856. The authors thank the E158 collaboration for their contribution to the target density fluctuation study data taking. Special thanks are given to P. Stiles for building the beam current monitor which is used for target heater feedback.

References

- [1] R. Carr et al., *A Precision Measurement of the Weak Mixing Angle in Møller Scattering*, SLAC-Proposal-E-158, July 17, 1997.
- [2] E. J. Beise et al., *A high power liquid hydrogen target for parity violation experiments*, Nucl. Instru. Methd. A 378 (1996) 383-391.
- [3] J. P. Chen, private communication, 2001.
- [4] J. G. Weisend II et al., *The Cryogenic System for the SLAC E158 Experiment*, Adv. Cryo. Engr. Vol. 47A. pp 171 -179 (2002).
- [5] R. Carr, *The E158 Target User's Guide*, 29 May, 2001.
- [6] R. Carr, J. Gao, C. E. Jones, and R. D. McKeown, *E158 Liquid Hydrogen Target Preliminary Design*, SLAC Internal Report E158-101, March 6, 2000.
- [7] R. Carr, J. Gao, C. E. Jones, and R. D. McKeown, *E158 Liquid Hydrogen Target Milestone Report*, April 21, 1999.
- [8] J. Gao, *E158 Cryogenic Target Control System*, January 29, 2001.
- [9] M. Woodley and M. Woods, *Skew Quad SQ27.5*, SLAC E158-TN #25, October 23, 2001.

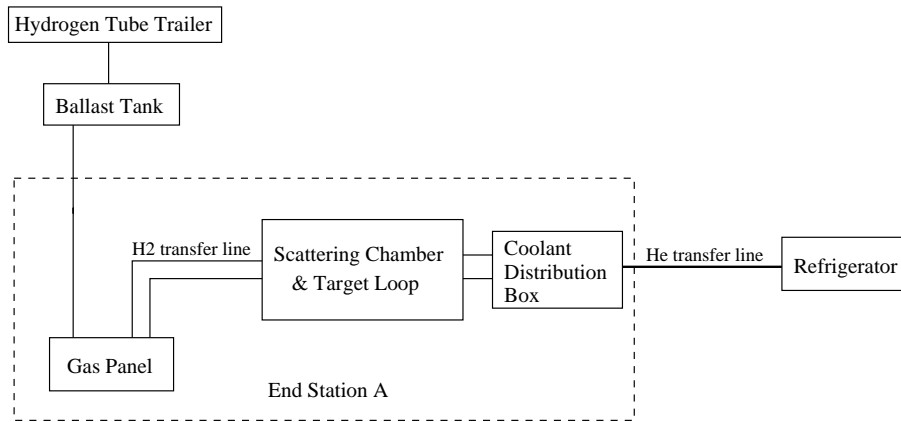


Fig. 1. Schematic of the E158 Target System

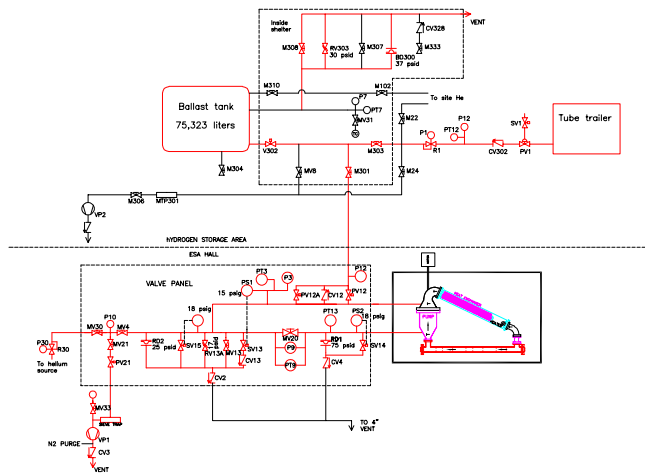


Fig. 2. Gas plumbing diagram.

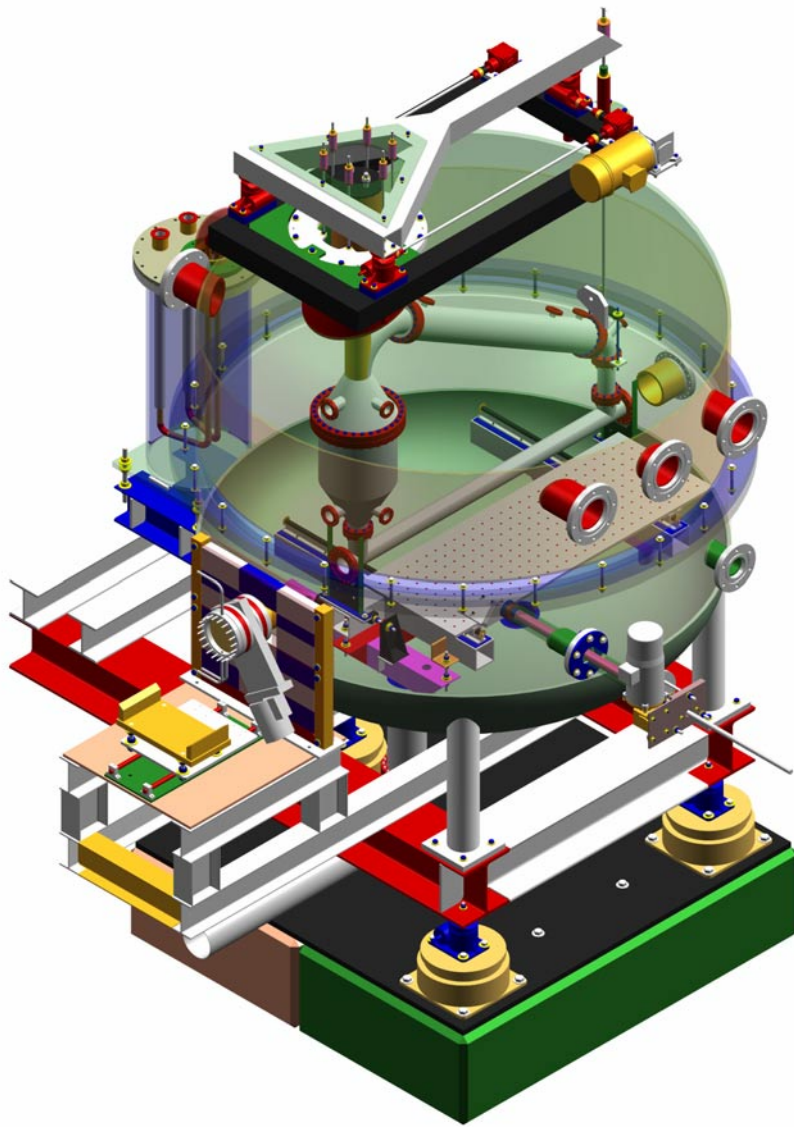


Fig. 3. A diagram of the scattering chamber that shows the target loop and its vertical motion mechanism.

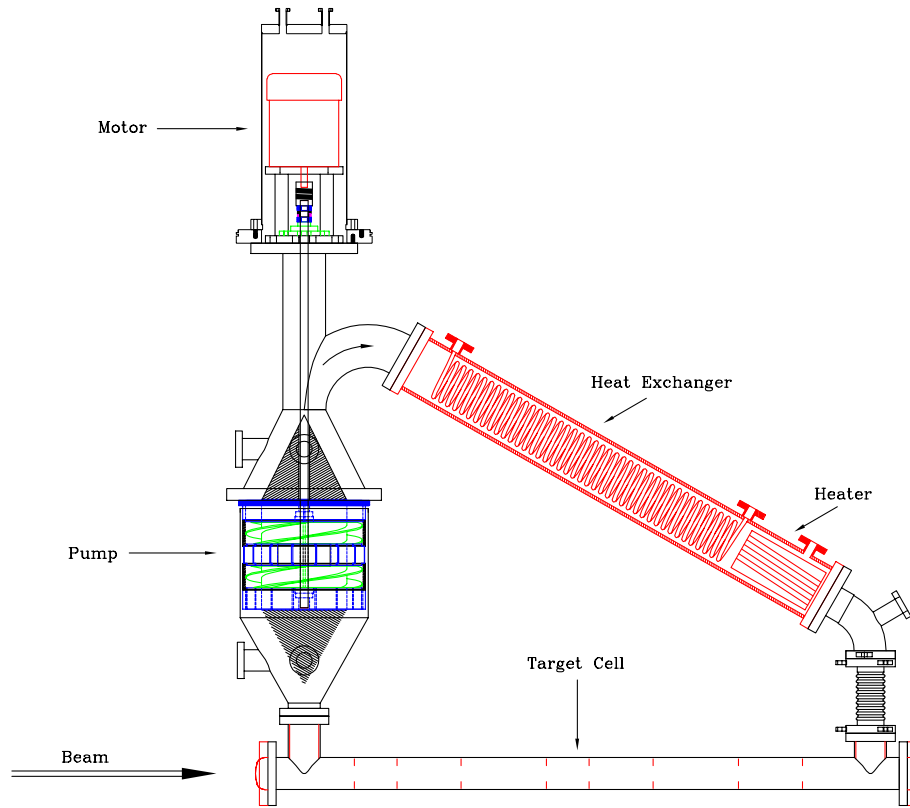


Fig. 4. Target loop diagram

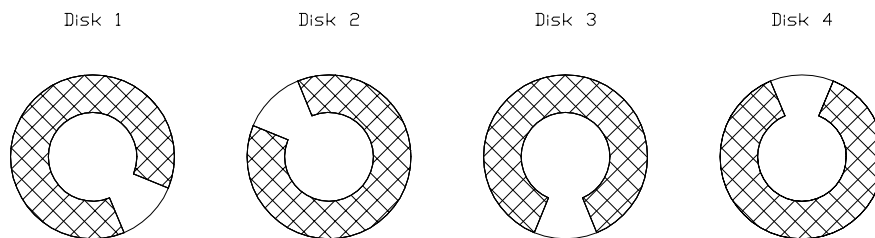


Fig. 5. Diagram of a set of the aluminum mesh discs. Two sets are installed in the target cell.

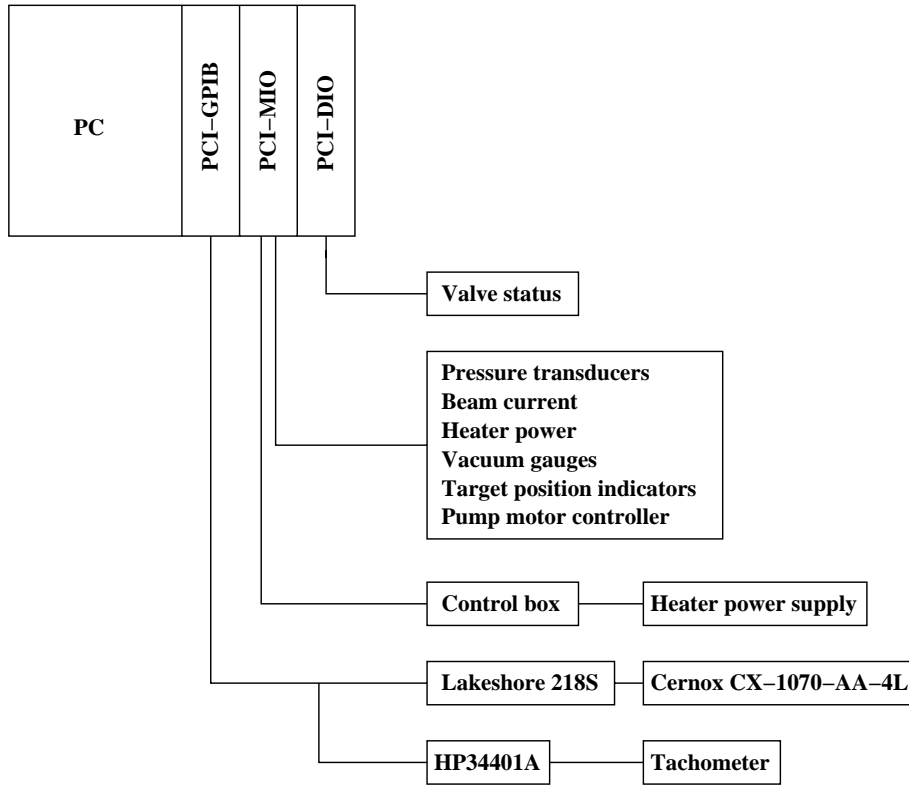


Fig. 6. Target control system.

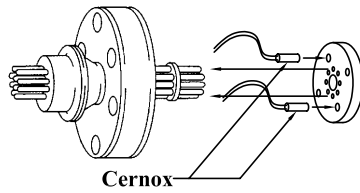


Fig. 7. Temperature sensor setup. From left to right: vacuum feedthrough, two Lakeshore Cernox sensors, and the sensor holder

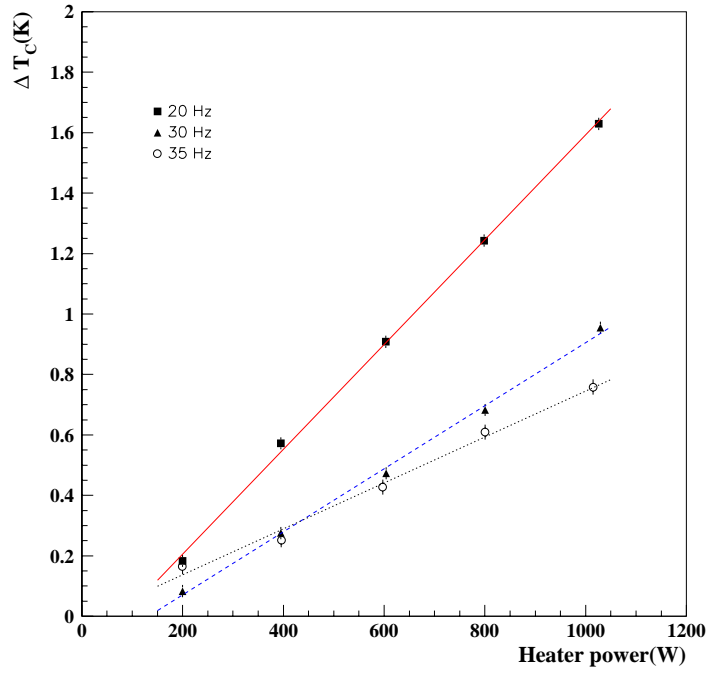


Fig. 8. ΔT_c for different pump speed and target heater power.

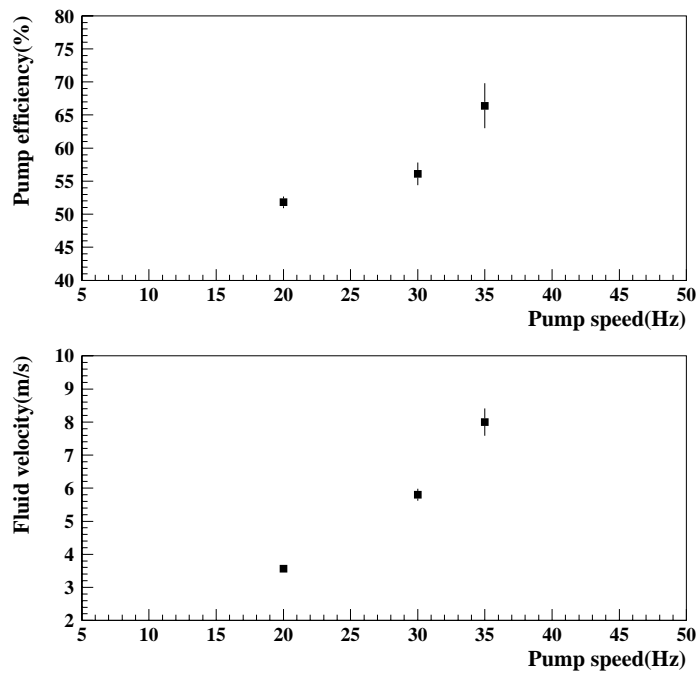


Fig. 9. Top figure: pump efficiency for different pump speed. Lower figure: longitudinal flow speed in the target cell for different pump speed.

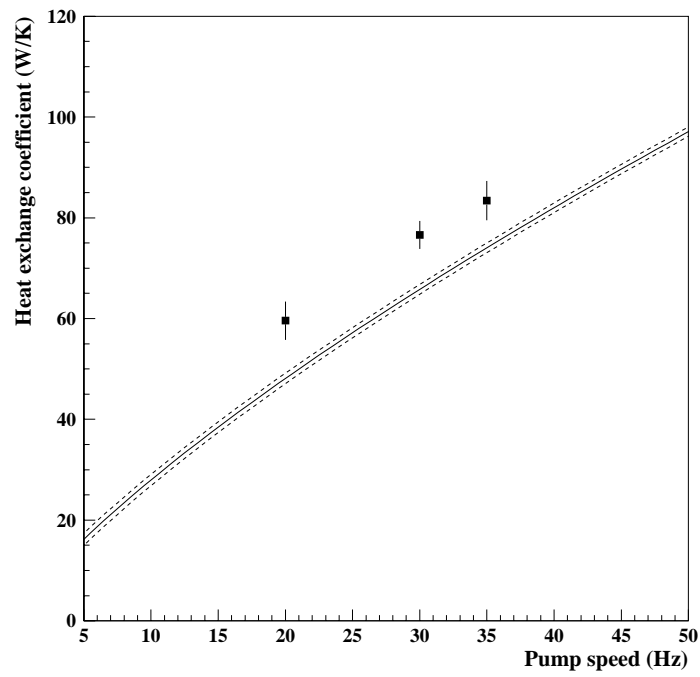


Fig. 10. Measured heat exchange coefficient vs. computed estimate. The dashed lines indicate the known uncertainty of the computation.

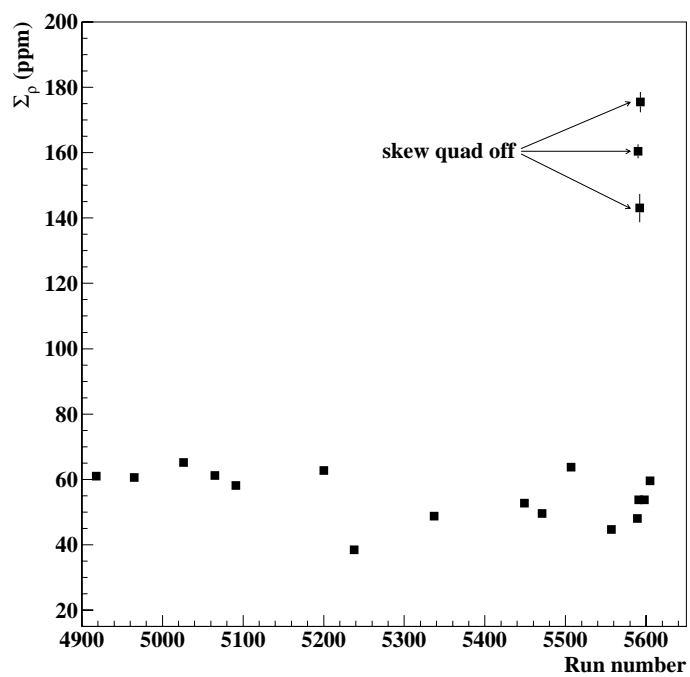


Fig. 11. Σ_ρ measured in different runs. Data were taken during the E158 physics run I. Except the three runs with skew quad [9] off, the rest are normal production runs.